DC-DC Converter for Gate Power Supplies with an Optimal Air Transformer

Christoph Marxgut*, Jürgen Biela*, Johann W. Kolar*, Reto Steiner† and Peter K. Steimer†
*Power Electronic Systems Laboratory, ETH Zurich
†ABB Switzerland Ltd., Power Electronics and MV Drives, Turgi, Switzerland
Email: marxgut@lem.ee.ethz.ch, www.pes.ee.ethz.ch

***Abstract*—Voltages in medium voltage (MV) systems as for example in MV drives, wind generation and smart grids are in the range of several kV. Hence, switches of medium power systems need gate drive power supplies which consider a galvanic isolation for safety reasons. In this paper a gate supply with a capacitive compensated air transformer for medium voltage systems is presented. This approach not only has the advantage of being capable in isolating almost arbitrarily high voltages but also is a compact, lightweight and cheap solution. The air transformer windings are realized as tracks on a circuit board (PCB). Furthermore, the air transformer has been optimized with respect to efficiency of the gate supply, which results in an optimal value of 85%. The optimization is accomplished by field simulation of the transformer and a circuit calculation to obtain the total losses. The simulation and optimization results are confirmed by a laboratory setup which is designed for an output voltage of 25 V at 100 W.**

I. Introduction

System voltages of medium high voltage systems are in the range of 1 kV to 52 kV. Hence, switches of medium high voltage converters are usually realized by IGBTs, IGCTs or thyristors because of their high voltage capabilities. Due to the high voltages the gates drive power supplies of these switches need to consider a proper galvanic isolation for safety reasons.

Today, most supply units use dry-type cast coil transformers as they are able to withstand high voltages. These transformers, however, are bulky, heavy, expensive and even small fabrication defects can result in a severe malfunction. Since the operating voltages in medium power systems tend to increase these problems are getting worse. Typical dimensions of dry-type cast coil transformers which are capable to withstand the stress of 20 kV_{rms} for 10 s without partial discharge are 20 cm × 20 cm × 20 cm at a weight of about 5.5 kg [1], [2].

To overcome these drawbacks a topology with a capacitive compensated air transformer can be applied [3]. Fig. 1 shows a press pack setup with gate drive unit which is supplied via an air transformer. It can be seen that this approach is compact, lightweight, stackable and cost efficient. The distance between primary and secondary winding determines the electric isolation capability of the gate power supply. However, the leakage inductance is increasing with an increase of the distance and hence capacitors on both the primary and the secondary winding are required to compensate the leakage [4]–[6]. In this paper air transformers with a distance of 20 mm between primary and secondary winding are considered. A

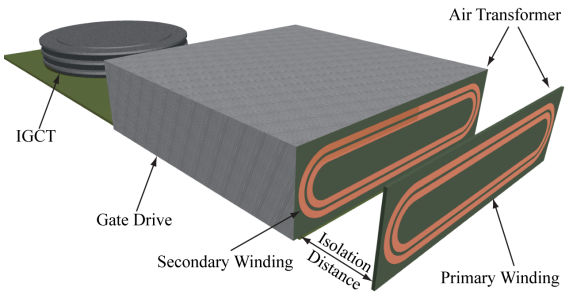

Fig. 1. IGCT setup with air transformer converter. The secondary compensation circuit and the diode rectifier can be integrated in the gate drive unit.

TABLE I
Converter Specifications

V_{in}	48 V_{DC}
V_{out}	25 V_{DC}
P_{out}	100 W
Isolation Distance	20 mm
Max. Dimensions	150 mm × 45 mm

setup with this distance is able to withstand 20 kV_{rms} without having any partial discharges [7] which was tested in [3]. Further improvement in high voltage isolation can be obtained if the windings are coated with a laminating layer. In [8] the interrelation between the air transformer's cross section area and the distance is given. It is pointed out that the diameter of a winding has to be at least as large as the distance. This limits the distance between primary and secondary winding for a given cross section area which is often determined by the gate drive unit's dimensions (cf. Fig. 1).

Since the ohmic losses in the air transformer are the major contribution to the total losses of the converter an efficiency optimization of the air transformer setup has been done. The optimization process will be discussed in **Section II**.
Another important issue regarding air transformers is the EMI compatibility. To improve the EMI behavior magnetic sheets are placed on top and bottom of the air transformer as will be discussed in **Section III**.

To confirm the proposed optimization of the converter

978-1-4244-4783-1/10/$25.00 ©2010 IEEE

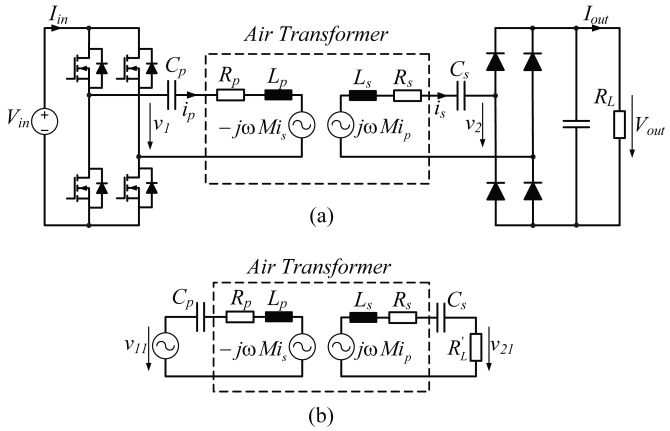

Fig. 2. (a) Circuit topology of the converter and (b) equivalent circuit for the fundamental component of the switching frequency.

system a laboratory setup has been build up which is shown in **Section IV**. The resonance circuit consisting of the resistive and inductive components of the air transformer as well as the compensation capacitors is fed by a full bridge inverter with a DC voltage V_{in} of 48 V and a switching frequency f_s of 400 kHz. The secondary voltage v_2 is rectified by a diode full bridge and an output capacitor. The circuit topology is shown in Fig. 2 (a). Typical values of gate drive power supplies are an output voltage of 25 V and an output power of 100 W. The converter specifications are given in Table I.

II. Efficiency Optimization

It is obvious that the air transformer represents the crucial element in this topology since the large leakage inductance and the winding resistances have major impact on the system behavior. Furthermore, a large primary current i_p, a large frequency ω and a large mutual inductance M would lead to a large secondary voltage as can be seen in the equivalent cirucit of the air transformer in Fig. 2 (a). The mutual inductance M is given by the transformer setup while the frequency is a degree of freedom. The primary current i_p can be maximized by decreasing the load of the input H-bridge which can be achieved by compensate the large primary inductance L_p by a capacitor C_p. To avoid a large voltage drop over the secondary leakage inductance a compensation capacitor C_s can be considered as well. This leads to a many parameters which have impact on the total efficiency of the DC-DC converter.

For that reason the electrical parameters of several air transformer designs have been evaluated. Based on these values the capacitors C_p and C_s are determined and a circuit calculation can be performed to obtain the system losses. This leads to an optimization loop of the gate supply.

The optimization process can be seen in Fig. 3. Starting point are the electrical specifications e.g. input and output voltages and the definition of the optimization space e.g. the maximum number of turns. Then an optimization loop starts which will be discussed in the following.

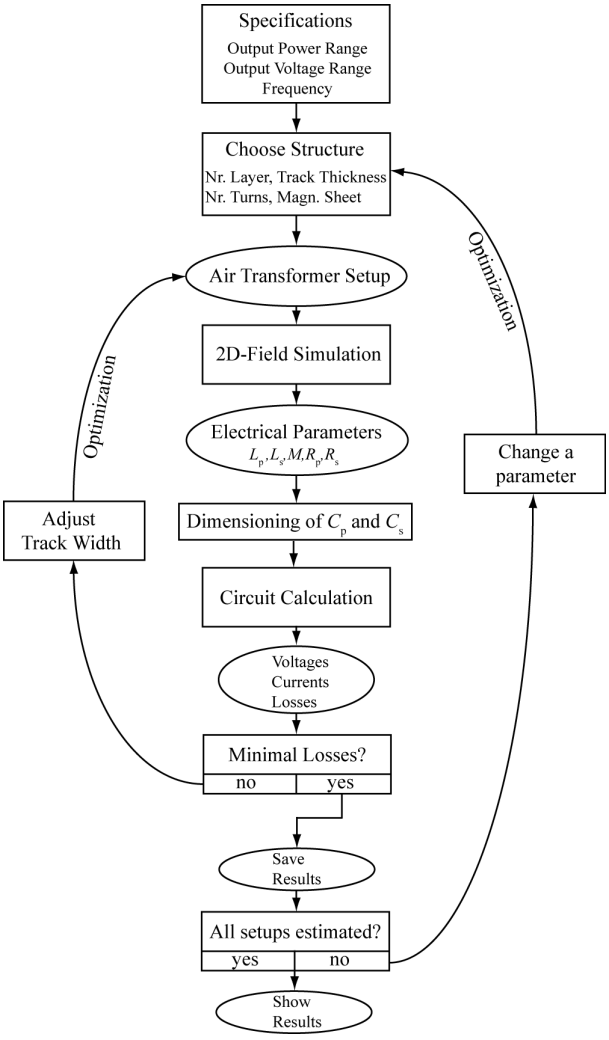

Fig. 3. Flow chart of the optimization process which starts with the electrical specifications and the limitations of the air transformer design parameters. Then for each setup an optimal track width with respect to efficiency is estimated. In the end the results are plottet to compare the setups.

A. Switching Frequency

The transfered power of an air transformer is proportional to the square of the switching frequency [4].

$$P = \Re\left\{\frac{\omega^2 M^2}{Z_s}\right\} \cdot i_p^2 \tag{1}$$

$$\text{whereas} \quad Z_s = R_s + j\omega(L_s - M) + \frac{1}{j\omega C_s} \tag{2}$$

Hence a high switching frequency leads to a good power transmission. On the other hand, a high frequency causes skin and proximity losses in the transformer windings. Furthermore, the gate drive losses increase. Therefore, in the following optimization a frequency of 400 kHz is chosen with is a trade-off between HF-losses and transmitted power. Switching losses can be neglected since soft switching is applied as will be discussed.

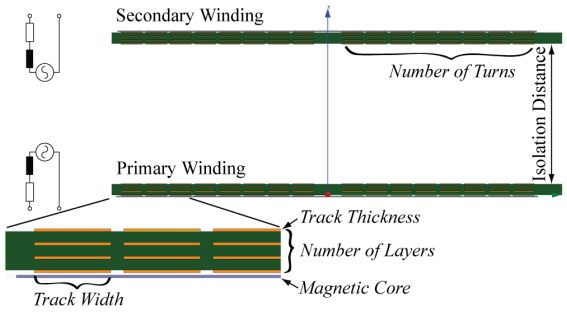

Fig. 4. Cross section of the air transformer with the design parameter: track width, track thickness, number of turns, number of layers and magnetic core material.

B. Design Parameters of the Air Transformer

Due to the high switching frequency the proximity effect and the skin effect in the windings are considerable. The number and position of tracks affect the AC resistance while the track width as well as the track thickness determine the DC resistance of the windings. To improve the magnetic properties of the transformer ferrite sheets can be placed on top of each winding.

So the number of layers, the number of turns, the track thickness, the track width as well as magnetic sheets are the optimization parameters as is indicated in Fig. 4. These parameters are varied in 2D field simulations which are performed with Maxwell by Ansoft in order to obtain the mutual inductance M, the primary and secondary inductance L_p and L_s as well as the winding resistances R_p and R_s for each setup. The winding resistances already consider skin and proximity effects.

To limit the optimization space the track thickness is considered as either 35 µm or 105 µm which are conventional copper thickness values. Furthermore, the air transformer is supposed to be symmetrical which means that primary and secondary windings are identically. The number of layers is limited to six for reasons of economy and the geometric size of the air transformer is limited to 150 mm × 45 mm with respect to conventional thyristor and IGCT gate drive dimensions (cf. Fig. 1).

C. Dimensioning of the Compensation Capacitors

The schematic in Fig. 2 can be classified in the input full bridge, the resonant circuit including the air transformer, and the output rectifier bridge.

The input H-bridge produces a square wave voltage v_1 with a maximum duty cycle D_{max}. A spectral decomposition of this voltage leads to its fundamental component which can be considered as an equivalent voltage source v_{11}.

$$v_{11} = \frac{4}{\pi} \cdot D_{max} \cdot V_{in} \tag{3}$$

If a large output capacitor is considered the output voltage V_{out} is constant and v_2 has nearly a square wave form. Considering only the fundamental component of voltage v_2 an equivalent resistance $R_L^{'}$ of the diode rectifier, the output capacitor and the load R_L can be evaluated [9].

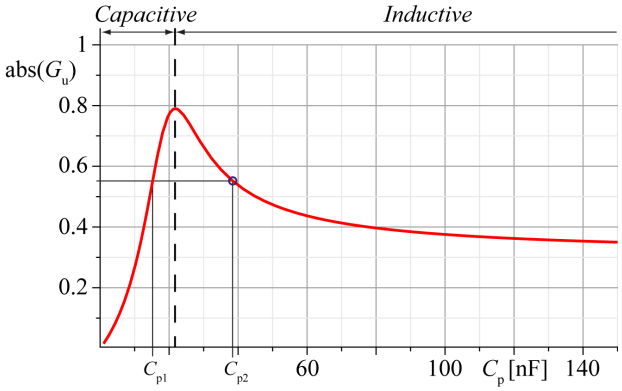

Fig. 5. Voltage transfer function G_u vs. capacitor C_p. It can be seen that two possible values for C_p would lead to the required voltage ratio. However, only the capacitor C_{p2} results in an inductive load to input H-bridge which enables ZVS.

$$v_{21} = \frac{4}{\pi} \cdot V_{out} \tag{4}$$

$$R_L' = \frac{8}{\pi^2} \cdot R_L \tag{5}$$

Hence the circuit in Fig. 2 (a) is simplified significantly as can be seen in Fig. 2 (b). Capacitor C_s on the secondary is chosen to be in resonance with the secondary leakage inductance L_s-M of the air transformer at the switching frequency f_s.

$$C_s = \frac{1}{(2\pi f_s)^2 \cdot (L_s - M)} \tag{6}$$

Consequently, the voltage transfer function depends only on the primary capacitor C_p for a given transformer setup and hence C_p can be calculated for the required output specifications.

$$G_u = \frac{v_{21}}{v_{11}} = \frac{\frac{s \cdot M \cdot R_L^{'}}{R_L^{'} + R_s + s \cdot M}}{R_p + s \cdot L_p + \frac{1}{s \cdot C_p} - \frac{s^2 \cdot M^2}{R_s + R_L^{'} + s \cdot M}} \tag{7}$$

In Fig. 5 the magnitude of the voltage transfer function G_u is shown as function of the primary capacitor C_p for a given parameter set. It can be seen that two solutions lead to the required voltage transfer ratio. If current i_p lags the voltage v_1 in Fig. 2 zero voltage switching (ZVS) of the H-bridge could be achieved. Consequently, it is beneficial to choose the capacitor C_p so that the H-bridge's load behavior is inductive. In Fig. 5 the border between inductive and capacitive behavior is indicated. C_{p2} has to be considered in order to achieve soft switching.

TABLE II
OPTIMIZATION RESULTS

				Min.Losses	Trackwidth
Air Core	2 Layer	35 µm	$N=4$	88.25 W	3.2 mm
	2 Layer	105 µm	$N=4$	28.60 W	3.2 mm
	4 Layer	35 µm	$N=1$	46.10 W	6.95 mm
	6 Layer	35 µm	$N=1$	25.33 W	13.45 mm
	6 Layer	105 µm	$N=1$	17.53 W	12.85 mm
Epcos C351	2 Layer	35 µm	$N=4$	56.10 W	3.65 mm
	2 Layer	105 µm	$N=4$	28.66 W	3.35 mm
μ_r **= 9**	4 Layer	35 µm	$N=1$	41.90 W	11.8 mm
σ **= 4 mS/m**	6 Layer	35 µm	$N=1$	23.80 W	14.35 mm
	6 Layer	105 µm	$N=1$	16.66 W	13.6 mm
TDK IRJ08	4 Layer	35 µm	$N=1$	31.70 W	13.3 mm
μ_r **= 100**	6 Layer	35 µm	$N=1$	22.20 W	16.05 mm
σ **= 4 mS/m**	6 Layer	105 µm	$N=1$	15.50 W	16.05 mm

D. Loss Calculation

Since all circuit elements are determined a circuit calculation can be performed to obtain the circuit voltages, currents and losses. Due to the band-pass filter behavior of the compensated air transformer sinusoidal currents i_p and i_s are considered. This approximation is confirmed by measurements. The loss calculation includes the conduction losses in the air transformer P_{at}, the conduction losses in the input H-bridge P_{hb} as well as in the output rectifier bridge P_{rb}.

$$P_{at} = R_p \cdot i_{p,rms}^2 + R_s \cdot i_{s,rms}^2 \tag{8}$$

$$P_{hb} = 4 \cdot (R_{DS(on)} \cdot i_{sw,rms}^2)$$

$$= 4 \cdot (R_{DS(on)} \cdot \frac{i_{p,rms}^2}{2}) \tag{9}$$

$$P_{rb} = 4 \cdot (V_{fw} \cdot i_{diode,av}) = 4 \cdot (V_{fw} \cdot \frac{I_{out}}{2}) \tag{10}$$

Here V_{fw} represents the forward voltage drop of the rectifier diodes.
Since soft switching is achieved no switching losses have to be considered. After the efficiency is calculated the track width is adapted until an optimal value is achieved. If an optimal track width is found either the number of turns or the number of layers is varied. The number of turns is limited by the maximum geometric dimensions of the transformer and the track width. The spacing between the tracks is kept constant at 0.5 mm. This procedure is done for an air transformer setup with no core sheet, Epcos C351 sheets ($\mu_r = 9$) [10] and TDK IRJ08 sheets ($\mu_r = 100$) [11]. A script file is written to automate the 2D simulation and the circuit calculation.

E. Optimization Results

The simulation results are presented in Fig. 6 and in Table II. Several air transformer designs lead to high resistances R_p and R_s so that the required voltage ratio can not be achieved. Therefore, these unfeasible setups are not shown in Fig. 6 and Table II but only those which achieve the voltage ratio. A further point of interest is that the optimal track width is equal for 35 µm and 105 µm. This can be explained by the fact that for six layers the proximity effect is irrelevant in the vertical direction (cf. Fig. 4). The skin depth of copper at a frequency $f_s = 400$ kHz is 104.5 µm. Hence, the resistance does not increase for this increase of the track thickness. Consequently, the simulation procedure has to be performed only for one track thickness.

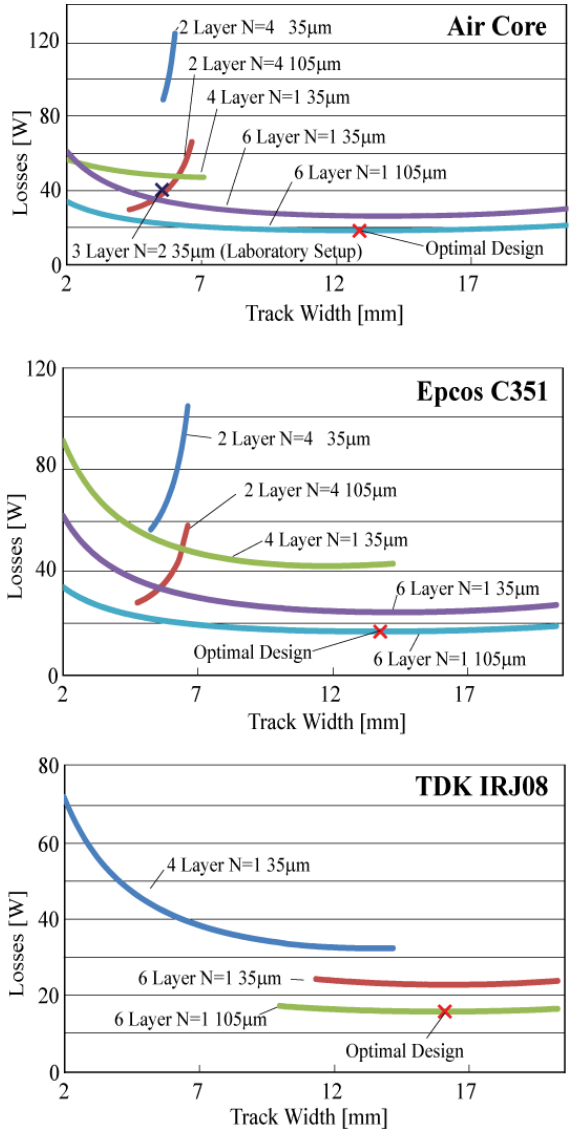

Fig. 6. Optimization Results.

It can be seen that the setup with 6 layers and 1 turn per layer is optimal and yields to minimal losses of 15.5 W. However, due to high manufacturing costs a suboptimal setup could be beneficial.

III. MAGNETIC PROPERTIES OF THE AIR TRANSFORMER

The core materials made by Epcos (C351) [10] and TDK (IRJ08) [11] differ in their relative permeability μ_r by a

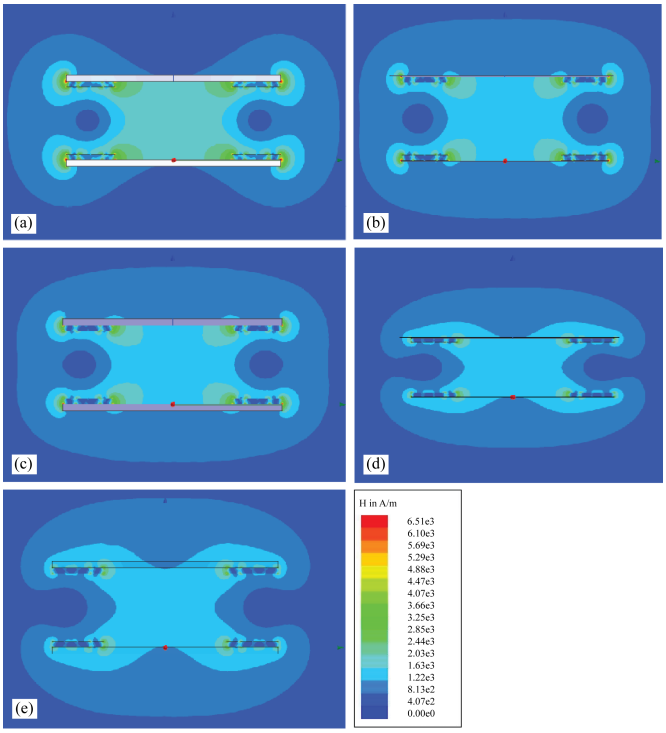

Fig. 7. Magnetic field plots for: (a) 2 mm TDK IRJ08, (b) 0.25 mm TDK IRJ08, (c) 2 mm Epcos C351, (d) 0.25 mm Epcos C351 on top and bottom of the PCB, (d) without core sheets.

factor of ten. It is obvious that materials which have a higher permeability improve the coupling factor of the transformer setup. Hence, concerning magnetic coupling the TDK sheet is better than the Epcos sheet. However, as can be seen in Table II for some setups the Epcos material achieves better results since a higher permeability also implies a higher flux density and hence higher eddy current losses.

Because of the large air gap the increase of magnetic coupling due to the magnetic sheets is marginal. However, the emitted field is reduced considerably with magnetic sheets. This can be seen in Fig. 7 where magnetic field plots are shown.

In Fig. 7 (a) and (b) the TDK sheet is placed on top and bottom of the air transformer with a thickness of 2 mm and 0.25 mm, respecively, whereas in (c) and (d) magnetic field plots for Epcos sheets with the same thicknesses are shown. A comparison to the air transformer setup without any core material which is shown in Fig. 7 (e) points out that the shielding effect of the TDK sheet with 2 mm thickness is superior to the other cases. In particular, the setup with 0.25 mm Epcos sheets shows almost no improvement compared to the pure air transformer setup. In general, thicker sheets result in better EMI shielding. The required foil thickness can be obtained by stacking several sheets.

IV. Laboratory Setup

To confirm the optimization results a laboratory setup was built. The air transformer setup consists of three layers with

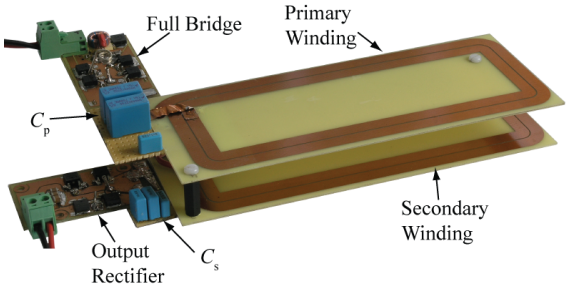

Fig. 8. Laboratory Setup whose parameters are given in Table III.

TABLE III
Air Transformer Parameters

Geometric Parameters	Electrical Parameters
Number of Layers: 6	L_p = 6.75 µH
Number of Turns: 2	L_s = 6.75 µH
Track Width: 6 mm	M = 2.21 µH
Track Thickness: 35 µm	R_p = 0.65 Ω
No Core Material	R_s = 0.65 Ω
Distance: 20 mm	

TABLE IV
Laboratory Setup Parameters

L_p = 6.75 µH	L_s = 6.75 µH
M = 2.21 µH	f_s = 400 kHz
R_p = 0.65 Ω	R_s = 0.65 Ω
C_p = 33.3 nF	C_s = 35 nF
MOSFETs - IR FR207Z	$R_{DS(on)}$ = 0.04 Ω
Diodes - IRP705G	V_{fw} = 0.65 V

each two turns. The track width is 6 mm and the track thickness is 35 µm. No core material is considered. This setup is not meant to be optimal as can be seen in Fig. 6 but is chosen due to its simple manufacturing. The simulation results can be seen in Table III while the setup is shown in Fig. 8. The measurement results for the given converter at an output power of 100 W can be seen in Fig. 9 (b) and a comparison with the simulated waveforms in Fig. 9 (a) shows good consistence. The input current i_p lags the input voltage v_1 so that soft switching is achieved. Furthermore, the sinusoidal approximation on which the loss calculation bases upon is justified. Electrical parameters of the setup are given in Table IV.

A breakdown of losses shows that the suboptimal air transformer causes 83 % of the total losses which can be seen in Fig. 10. The full bridge inverter and the diode rectifier generate 5 % and 12,% of the losses, respectively. Consequently, the optimal air transformer design is crucial for a good overall efficiency. The difference between calculation and measurment can be explaind by the fact that gate drive losses and losses in the auxiliary supply as well as high frequency current losses are not considered in the loss calculation. In Fig. 10 the breakdown of losses is shown for the optimal transformer setup. As can be seen the distribution of losses is more balanced. The losses in the diode rectifier bridge are constant

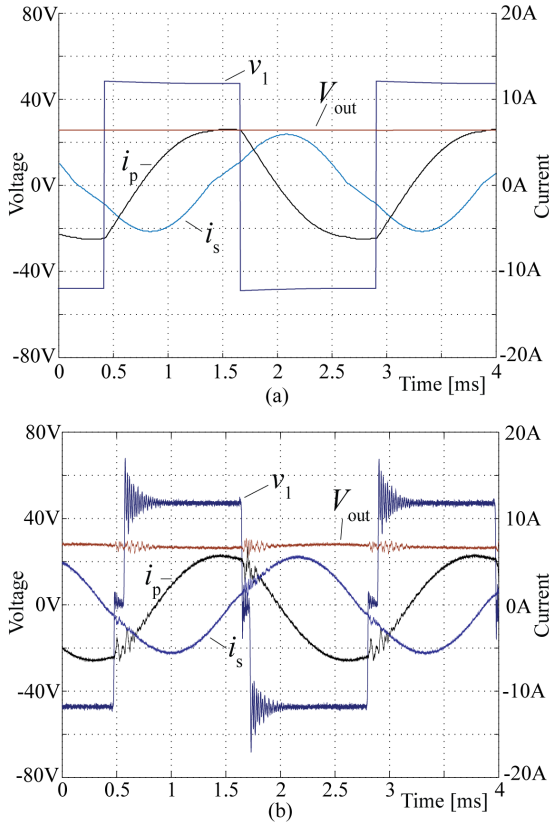

Fig. 9. (a) Circuit Simulation and (b) Measurement Results.

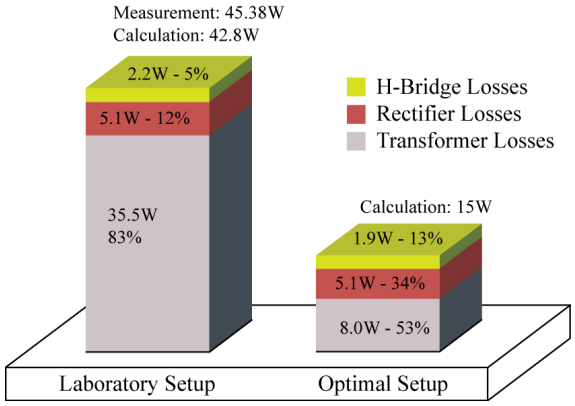

Fig. 10. Breakdown of losses for the laboratory setup and the optimal setup for an output voltage V_{out} of 25 V and an output power P_{out} of 100 W.

since the output voltage and the output power is constant for both setups. The losses in the H-bridge decrease slightly since the primary current i_p which is required to transfer the power to the load decreases.

V. Conclusion

In this paper an isolated gate drive power supply for medium high voltage switches is presented. The electric isolation is realized by an air transformer whose distance between primary and secondary winding withstand the high voltages. In this paper a distance of 20 mm between primary and secondary is considered which would withstand system voltages of 20 kV_{RMS} which is shown in [3]. Since the air transformer is responsible for the main part of the losses an optimization is performed to improve the converter efficiency. The optimization is accomplished by field simulations of several air transformer setups followed by a cirucuit calculation in which the compensation capacitors are obtained. After that the efficiency is calculated and the parameters are changed which is the initiation of a new calculation cycle. The optimization results shows that an overall efficiency of over 85 % at rated load can be obtained if a proper air transformer setup is chosen. The optimization method is confirmed by a laboratory setup.

This topology would further allow a gate signal transmission over the air transformer which would combine the isolation of the power supply and signal path. Hence a compact and cheap solution is obtained where the good galvanic isolation would also be applied for the gate signal.

References

[1] "Siebel & scholl GmbH." http://www.siebel-scholl.de/index.html.

[2] A. van den Bossche and V. C. Valchev, *Inductors and Transformers for Power Electronics*. CRC, 1 ed., Mar. 2005.

[3] R. Steiner, P. K. Steimer, F. Krismer, and J. W. Kolar, "Contactless energy transmission for an isolated 100 W gate driver supply of a medium voltage converter," *Industrial Electronics, 2009. IECON 2009. 35th Annual Conference of IEEE*, no. 4, 2009.

[4] C. Wang, O. Stielau, and G. Covic, "Design considerations for a contactless electric vehicle battery charger," *Industrial Electronics, IEEE Transactions on*, vol. 52, no. 5, pp. 1308–1314, 2005.

[5] O. Stielau and G. Covic, "Design of loosely coupled inductive power transfer systems," in *Power System Technology, 2000. Proceedings. PowerCon 2000. International Conference on*, vol. 1, pp. 85–90 vol.1, 2000.

[6] X. Liu and S. Hui, "Optimal design of a hybrid winding structure for planar contactless battery charging platform," in *Industry Applications Conference, 2006. 41st IAS Annual Meeting. Conference Record of the 2006 IEEE*, vol. 5, pp. 2568–2575, 2006.

[7] W. Zaengl, S. Yimvuthikul, and G. Friedrich, "The temperature dependence of homogeneous field breakdown in synthetic air," *Electrical Insulation, IEEE Transactions on*, vol. 26, no. 3, pp. 380–390, 1991.

[8] E. Waffenschmidt and T. Staring, "Limitation of inductive power transfer for consumer applications," in *Power Electronics and Applications, 2009. EPE '09. 13th European Conference on*, pp. 1–10, 2009.

[9] R. Erickson and D. Maksimovic, *Fundamentals of Power Electronics*. Springer, 2nd ed., 2001.

[10] "Epcos AG." http://www.epcos.com.

[11] "TDK corporation." http://www.tdk.com.